Atmos. Chem. Phys. Discuss., 13, 32291–32325, 2013
www.atmos-chem-phys-discuss.net/13/32291/2013/
doi:10.5194/acpd-13-32291-2013


Atmospheric Chemistry and Physics Discussions
Open Access



# Incorporation of advanced aerosol activation treatments into CESM/CAM5: model evaluation and impacts on aerosol indirect effects

**B. Gantt[1,*], J. He[1], X. Zhang[1], Y. Zhang[1], and A. Nenes[2,3]**

[1]Department of Marine, Earth, and Atmospheric Sciences, North Carolina State University, Raleigh, NC, USA
[2]School of Earth and Atmospheric Sciences, Georgia Institute of Technology, Atlanta, GA, USA
[3]School of Chemical and Biomolecular Engineering, Georgia Institute of Technology, Atlanta, GA, USA
[*]now at: Atmospheric Modeling and Analysis Division, National Exposure Research Laboratory, US Environmental Protection Agency, Research Triangle Park, NC, USA

Received: 15 October 2013 – Accepted: 27 November 2013 – Published: 10 December 2013

Correspondence to: Y. Zhang (yang_zhang@ncsu.edu)

Published by Copernicus Publications on behalf of the European Geosciences Union.

## Abstract

One of the greatest sources of uncertainty in the science of anthropogenic climate change is from aerosol-cloud interactions. The activation of aerosols into cloud droplets is a direct microphysical link between aerosols and clouds; parameterizations of this process realistically link aerosol with cloud condensation nuclei (CCN) and the resulting indirect effects. Small differences between parameterizations can have a large impact on the spatiotemporal distributions of activated aerosols and the resulting cloud properties. In this work, we incorporate a series of aerosol activation schemes into the Community Atmosphere Model version 5.1.1 within the Community Earth System Model version 1.0.5 (CESM/CAM5), which include factors such as insoluble aerosol adsorption, giant cloud condensation nuclei (CCN) activation kinetics, and entrainment to understand their individual impacts on global scale cloud droplet number concentrations (CDNCs). Compared to the existing simple activation scheme in CESM/CAM5, this series of schemes predict CDNCs that are typically in better agreement with satellite-derived and observed values. The largest changes in predicted CDNCs occur over desert and oceanic regions, owing to the enhanced activation of dust from insoluble aerosol adsorption and reductions in cloud supersaturation from the intense absorption of water vapor in regions of strong giant CCN emissions (e.g., sea-salt). Comparison of CESM/CAM5 against satellite-derived cloud optical thickness and liquid water path shows that the updated activation schemes improve the low biases in their predictions. Globally, the incorporation of all updated schemes leads to an average increase in column CDNCs of 155 %, an increase in shortwave cloud forcing of 13 %, and a decrease in surface shortwave radiation of 4 %. In terms of meteorological impacts, these updated aerosol activation schemes result in a slight decrease in near-surface temperature of 0.9 °C and precipitation of 0.04 mm $day^{-1}$, respectively. With the improvement of model-predicted CDNCs and better agreement with most satellite-derived cloud properties, the inclusion of these aerosol activation processes should result in better predictions of the aerosol indirect effects.





ACPD
13, 32291–32325, 2013

## 1 Introduction

Radiative forcing of climate by aerosols is among the most uncertain aspects of anthropogenic climate change (Intergovernmental Panel on Climate Change, IPCC; Forster et al., 2007). By serving as cloud condensation nuclei (CCN), anthropogenic aerosols can increase droplet number concentration and enhance the albedo of liquid-phase clouds (Twomey, 1974, 1977). In reducing droplet size, anthropogenic CCN can inhibit drizzle production under certain conditions and lead to increased liquid water content, cloud lifetime, and cloud albedo (Albrecht, 1989). These two aerosol-cloud interactions are known as the cloud albedo (or first indirect) and lifetime (or second indirect) effects, respectively, and together constitute the aerosol indirect effect (Forster et al., 2007). An important aspect of aerosol-cloud interactions involves the process of aerosol activation into droplets (also referred to as droplet nucleation), which describes the growth of aerosols into cloud droplets. Although Köhler theory (Köhler, 1936) accurately predicts the activation of particles at a given maximum supersaturation, it is the determination of the maximum supersaturation that is the greatest source of uncertainty (Ghan et al., 2011). The earliest representations of droplet nucleation in climate models used empirical relationships between CDNC and sulfate mass concentration (Boucher and Lohmann, 1995) or aerosol number concentration (Jones et al., 1994). Despite relatively strong relationships between CDNC and these aerosol parameters in several environments (Leaitch et al., 1992; Martin et al., 1994; Ramanathan et al., 2001), the empirical relationships do not explicitly account for the dependence of the droplet nucleation on aerosol size distribution, aerosol composition, or updraft velocity and therefore are limited in their ability to accurately predict CDNC on a global scale.

Physically-based parameterizations of aerosol activation or droplet nucleation are designed to quickly provide the number of aerosols activated into cloud droplets as a function of the aerosol number size distribution, chemical composition, and environmental conditions. One of the most widely-used parameterizations describing aerosol activation, Abdul-Razzak and Ghan (2000) (hereto referred as AR-G00), is based on the work of Abdul-Razzak et al. (1998) and derives an empiric calculation of the maximum supersaturation by using values based on the regression of numerical parcel calculations. By parameterizing aerosol activation in terms of a critical supersaturation (Twomey, 1959) and critical radius within a lognormal aerosol size distribution (Ghan et al., 1993), Abdul-Razzak et al. (1998) obtained an activation parameterization in terms of all of the parameters of the aerosol size distribution whose activated fraction is within 10 % difference from that of a numerical model for most conditions. AR-G00 updated Abdul-Razzak and Ghan (1998) (which applied to a signal lognormal aerosol mode with uniform chemical composition) by enabling its application to an aerosol population represented by lognormal modes, each with a uniform bulk hygroscopicity determined by an internal mixture of chemical components within each mode. As air quality and climate models often characterize aerosols by multiple lognormal modes, AR-G00 has been widely included in many models (see Table 3 in Ghan et al. (2011) for summary).

Another widely-used activation parameterization, Fountoukis and Nenes (2005) (hereto referred as FN05), is based on Nenes and Seinfeld (2003) and includes explicit calculations of mass transfer, condensation coefficient, integration over the aerosol size distribution, and kinetic limitations. In order to maintain computational efficiency, the parameterization of Nenes and Seinfeld (2003) split the aerosol population (defined in terms of a sectional size distribution) into two groups: (1) those with diameters which activate near the maximum supersaturation and (2) those with diameters which do not activate near the maximum supersaturation. FN05 updated this parameterization to account for a lognormal aerosol size distribution and size-dependent mass transfer coefficient of water vapor to droplets; it also addresses some of the limitations of AR-G00, especially for conditions when kinetic limitations on droplet nucleation are expected. When strong kinetic limitations occur, the maximum supersaturation is not the same as the critical supersaturation (defined as the saturation at which a particle radius will grow beyond the equilibrium size at the maximum supersaturation). Under these conditions, the relationship between maximum and critical supersaturation is determined empir-





ACPD
13, 32291–32325, 2013

ically in FN05 from numerical simulations for a range of conditions. Another unique feature of FN05 is its ability to account for the influence of gas kinetics on the water vapor diffusivity. This influence depends on particle size and on the value of the condensation coefficient. Fountoukis and Nenes (2005) found that an average value of the diffusivity over an appropriate size range can account for the influence of gas kinetics on droplet nucleation. By expressing the solution in terms of the condensation coefficient, FN05 is applicable to a range of environmental conditions. Unlike AR-G00, FN05 does not approximate functions of the maximum supersaturation and does not rely on empirical relationships (except in the case of strong kinetic limitations across the CCN population). A disadvantage of FN05 is that it requires iterations to solve for maximum supersaturation which makes it more computationally expensive than AR-G00 (Ghan et al., 2011). A comprehensive comparison of AR-G00, FN05, and several other activation parameterizations was performed by Ghan et al. (2011), which showed that FN05 predicted the number fraction of activated aerosol more consistent with that of a high-confidence numerical solution. Despite their many differences, the implementation of both AR-G00 and FN05 in CAM5.0 resulted in a small difference (0.2 $W m^{-2}$, 10 %) in the predicted effect of anthropogenic aerosol on shortwave cloud forcing (Ghan et al., 2011). This study expands upon the work of Ghan et al. (2011) by evaluating the individual processes affecting aerosol activation within an Earth Systems Model with advanced chemistry and aerosol treatments using global scale satellite/ground-base observations. Our objective is to improve the model's representation of aerosol-cloud interactions by incorporating advanced aerosol activation treatments into the Community Atmosphere Model version 5.1.1 within the Community Earth System Model version 1.0.5 (hereto referred as CESM/CAM5) and demonstrating the benefits of such advanced treatments through an initial application of the improved model.



Discussion Paper | Discussion Paper | Discussion Paper | Discussion Paper |

ACPD

13, 32291–32325, 2013

Incorporation of advanced aerosol activation treatments into CESM/CAM5

B. Gantt et al.

## 2 Model setup

### 2.1 CESM/CAM5 with an advanced aerosol activation module

In this work, we use CESM/CAM5 to explore the impact of several different aerosol activation schemes on global scale cloud properties and meteorology through aerosol-cloud interactions. The CESM/CAM5 used in this work is a version recently released by NCAR and further developed and improved at North Carolina State University (NCSU) (He and Zhang, 2013). It includes advanced gas-phase chemistry, aerosol nucleation, and inorganic aerosol thermodynamics that are coupled with the 7-mode modal aerosol module (MAM7) in CAM5. The gas-phase chemistry is based on the 2005 Carbon Bond chemical mechanism with global extension (CB05_GE) (Karamchandani et al., 2012). The aerosol nucleation is based on a combination of the default nucleation parameterizations of Vehkamaki et al. (2002) and (Merikanto et al., 2007) and a newly added ion-mediated aerosol nucleation (Yu, 2010) above the planetary boundary layer (PBL), as well as a combination of the three and an additional parameterization of Wang et al. (2009) in the PBL. The inorganic aerosol thermodynamics is based on ISORROPIA II of (Fountoukis and Nenes, 2007) that explicitly simulates thermodynamics of $SO_4^{2-}$, $NH_4^+$, $NO_3^-$, $Cl^-$, and $Na^+$ as well as the impact of crustal species associated with the fine dust mode. Other updates in the CESM/CAM5 version used in this work include the splitting sea-salt aerosol in MAM7 into sodium and chloride to enable chlorine chemistry in ISORROPIA II and addition of aqueous-phase dissolution and dissociation of $HNO_3$ and HCl. In addition, while the released version of MAM7 uses a constant mass accommodation coefficient of 0.65 for all condensable species, the NCSU's version uses species-dependent accommodation coefficients for $H_2SO_4$, $NH_3$, $HNO_3$, and HCl, with the value of 0.02, 0.097, 0.0024, and 0.005, respectively.

In the released version of CESM/CAM5, aerosol activation occurs if liquid condensate is present and the number of cloud droplets decreases below the number of active CCN diagnosed by the AR-G00 scheme as a function of aerosol chemical and physical parameters (as given by MAM7 in this case), temperature, and vertical velocity (Neale





ACPD
13, 32291–32325, 2013

et al., 2010). Stratiform cloud microphysics are described by Morrison and Gettelman (2008), which treats both the cloud droplet number concentration and mixing ratio in order to simulate indirect aerosol effects and cloud-aerosol interactions. In this work, the NCSU's version of CESM/CAM5-MAM7 is further developed by providing an alternative to the AR-G00 scheme with FN05 and the updates of Kumar et al. (2009) (K09), Barahona et al. (2010) (B10), and Barahona and Nenes (2007) (BN07) to FN05, which account for adsorption activation from insoluble CCN, giant CCN equilibrium timescale on aerosol activation, and the effects of entrainment, respectively. In the K09 parameterization, water vapor is adsorbed onto insoluble particles such as dust and black carbon (BC) whose activity is described by a multilayer Frenkel–Halsey–Hill (FHH) adsorption isotherm. Calculations of the FHH adsorption isotherm in K09 account for particle curvature with atmospherically-relevant adsorption parameters. Values of 2.25 and 1.20 are used for the $A_{FHH}$ and $B_{FHH}$ empirical constants, respectively (where $A_{FHH}$ characterizes the interactions of adsorbed molecules with the aerosol surface and adjacent adsorbate molecules and $B_{FHH}$ characterizes the attraction between the aerosol surface and the adsorbate in subsequent layers (Kumar et al., 2009)). As insoluble adsorption leads to the activation of some particles which would not easily activate under Köhler theory, a regional increase in the CDNC is expected in clouds affected by high dust or BC concentrations. As FHH adsorption activation occurs in addition to Köhler activation in our version of CESM/CAM5, decreases in CDNC should be rare. The B10 parameterization accounts for the slow condensation upon inertially-limited (large) droplets in the calculation of the droplet surface area and maximum supersaturation in a cloud updraft. As the slow condensation (relative to cloud formation timescales) limits the activation of giant CCN, a regional decrease in the CDNC is expected in clouds affected by large sea-salt aerosol and aged-dust concentrations. BN07 parameterizes the impact of entrainment on aerosol activation by assuming homogeneous mixing of the rising air parcel and dry ambient air at a timescale much faster than that of aerosol activation and introducing the concept of critical entrainment where the entrainment is strong enough to prevent aerosol activation. As entrainment reduces the supersatura-





ACPD
13, 32291–32325, 2013

tion of the rising air parcel, inclusion of the BN07 scheme is expected to more realistically simulate the decrease in CDNC in air parcels with strong entrainment (i.e., regions with deep convection). In the BN07 parameterization implemented in CESM/CAM5, the entrainment rate is calculated using the updraft entrainment rate derived from the deep convection scheme (Zhang and McFarlane, 1995) within CESM/CAM5. The critical entrainment in the BN07 parameterization is calculated by assuming that the difference between parcel and ambient temperature is zero, which maximizes the potential impact of entrainment on cloud droplet formation (Barahona and Nenes, 2007). The simulations with the FN05 scheme and updates use the same interface as that of AR-G00, with an accommodation coefficient value of 0.06 (Fountoukis and Nenes, 2005) and an insoluble fraction of each mode calculated from its hygroscopicity parameter (Petters and Kreidenweis, 2007).

### 2.2 Model simulation design and setup

The CESM/CAM5 baseline simulations are performed using AR-G00 and FN05 for aerosol activation. In addition, four sensitivity simulations are designed to test individually and then collectively the impact of the aforementioned FFN05-based updated parameterizations on global cloud properties, meteorology, and aerosol indirect effects. During the first three simulations, FN05 is updated individually by K09, B10, and BN07 (referred to as FN05/K09, FN05/B10, and FN05/BN07, respectively). The last simulation contains FN05 with all three updates (referred to as FN05/K09/B10/BN07). Table 1 summarizes all the simulations completed in this work along with their purposes.

All CESM/CAM5 simulations are performed for the year 2001 with a 3 month spin-up at a horizontal grid resolution of $0.9^\circ \times 1.25^\circ$. The initial meteorological conditions are generated using the component set of CESM, B_1850–2000_CAM5_CN, which includes all active components of CESM, 1850 to 2000 transient climate, CAM5 physics, and carbon/nitrogen cycling in the Community Land Model. The initial chemical conditions are based on those available in the default MOZART. One-year spin up period is used to create initial conditions for the missing species. Anthropogenic emissions





ACPD
13, 32291–32325, 2013

and dimethyl sulfide (DMS) emissions are based on the inventory used for the global-through-urban weather and forecasting model with chemistry (GU-WRF/Chem) simulations in Zhang et al. (2012) and with scaled emissions of sulfur dioxide ($SO_2$), ammonia ($NH_3$), BC, and organic carbon (OC) in the continental US, Europe, and east Asia domains based on several recent emission inventories, known uncertainties in those emissions, and initial model evaluation using available observations of surface chemical concentrations (He and Zhang, 2013). Online natural emissions include biogenic volatile organic compounds based on the Model of Emissions of Gases and Aerosols from Nature (MEGAN) scheme version 2 (Guenther et al., 2006; Heald et al., 2008), dust based on the Dust Entrainment and Deposition scheme of Zender et al. (2003), and sea-salt aerosol based on Mårtensson et al. (2003) for particles $< 2.8\,\mu m$ in dry diameter and Monahan et al. (1986) for particles $\geq 2.8\,\mu m$ in dry diameter.

### 2.3 Model evaluation datasets and protocol

Model performance is evaluated for both radiative and meteorological predictions from available surface and satellite observations for the year 2001, including aerosol optical depth (AOD), CDNC, cloud fraction (CF), cloud optical thickness (COT), liquid water path (LWP), shortwave cloud forcing (SWCF), downward shortwave radiation (SWDOWN), downward longwave radiation (LWDOWN), outgoing longwave radiation (OLR), temperature at 2 m (T2), wind speed at 10 m (WS10), and total daily precipitation. Satellite datasets are derived from the Moderate Resolution Imaging Spectroradiometer (MODIS) collection 5.1 and the Clouds and Earth's Radiant Energy System (CERES) sensors aboard the Terra satellite. Global surface radiation data is from the Baseline Surface Radiation Network (BSRN). T2 is evaluated using the National Climatic Data Center (NCDC) and the National Centers for Environmental Prediction-Department of Energy (NCEP-DOE) Reanalysis-2 dataset. WS10 is evaluated using the NCDC data. Precipitation is evaluated using both the NCDC and Global Precipitation Climatology Project (GPCP) datasets. In addition to the MODIS-derived CDNC (Bennartz, 2007), a dataset of CDNC compiled mostly from field campaigns (Karydis





ACPD
13, 32291–32325, 2013

et al., 2011) is included. CDNC is calculated as an average value of layers between 960 to 850 mb for comparison with the satellite-derived values of Bennartz (2007) and is extracted for the 930 mb layer (near the top of the boundary layer) for comparison with the dataset from Karydis et al. (2011) and references therein. The protocols for performance evaluation follow those used in Zhang et al. (2012), focusing on the annual-averaged normalized mean bias (NMB) and correlation coefficient.

## 3 Results

### 3.1 Global performance statistics

Table 2 summarizes model performance statistics for radiative and meteorological predictions of CESM/CAM5 with various aerosol activation schemes over the global domain. AOD is underpredicted by all simulations, with little change in the NMBs (ranging from −34.0 to −30.8 %) and correlations (~ 0.64) among the simulations. The underprediction of AOD is likely due to both underpredictions of terrestrial/anthropogenic aerosol concentrations (He and Zhang, 2013) and overestimates of oceanic AOD in the MODIS collection 5.1 (Levy et al., 2013). The small change in AOD among all simulations is likely due to changes in meteorological parameters such as surface winds (which strongly affects the online emissions of sea-salt aerosol and dust) and precipitation (which affects the aerosol wet deposition) resulted from chemistry feedbacks to meteorology through various direct and indirect effects (Zhang, 2008). Compared to AR-G00, all of the FN05 series of simulations have the same or higher average wind speed (reflected by its lower underpredictions in Table 2) and lower average precipitation rate (reflected by its lower overpredictions in Table 2).

CNDC, on the other hand, is strongly influenced by the selection of aerosol activation scheme. The AR-G00 simulation gives NMBs of −40.8 and −71.7 % for the satellite-derived and in-situ observations, respectively. For comparison, the CDNCs for the FN05 simulations and all sensitivity simulations with updated activation treatments are either less underpredicted or become overpredicted with NMBs of 10.2 to 37.4 % and −40.6 to −21.5 % for the satellite-derived and in-situ observations, respectively. The higher CDNC predicted by the FN05 simulation relative to AR-G00 is consistent with results from Ghan et al. (2011) and Zhang et al. (2012), who attributed the difference to the tendency of the FN05 scheme to diagnose higher activation fractions than the AR-G00 scheme for most conditions. The higher activation fraction in FN05 relative to AR-G00 is primarily due to the different values of the effective uptake coefficient used in FN05 (0.06) and AR-G00 (1.0 or higher) (Zhang et al., 2012). The general improvement in CDNC predictions (relative to observations) from the FN05 scheme is also consistent with the Ghan et al. (2011) results, showing that the FN05 activated fraction is more similar than that of AR-G00 to a numerical solution for marine, clean continental, and background aerosol distributions for a range of updraft velocities. Compared to the satellite-based CDNC dataset, FN05/K09 has the highest overprediction and FN05/B10 has the lowest overprediction among the all FN05-based simulations. These trends are expected, as insoluble adsorption in FN05/K09 leads to additional activation in regions with high dust/BC concentrations while giant CCN activation kinetics leads to less activation in regions with high dust/sea-salt concentrations. The inclusion of entrainment in FN05/BN07 results in little change in the CDNC from the FN05 scheme, possibly due to feedbacks between aerosol activation and cloud microphysical processes during deep convection. Areas of deep convection have previously been identified as having a nonlinear relationship between enhanced aerosol concentration (and activation) and cloud microphysics that is dependent on meteorological parameters (Khain et al., 2008; Rosenfeld et al., 2008). Among the three processes (insoluble adsorption, giant CCN activation kinetics, and entrainment) updated in the FN05 scheme, giant CCN activation kinetics in FN05/B10 seems to be the most dominant, leading to the largest changes from the predictions by FN05 and dominating the changes in CDNC predictions caused by the three updates in the FN05/K09/B10/BN07 simulation. Correlations between the satellite-derived/in-situ observed CDNCs and CESM/CAM5 predictions improve from AR-G00 to the FN05 series of simulations (with correlations





ACPD
13, 32291–32325, 2013

of 0.49 to 0.55–0.60 and 0.03 to 0.10–0.39 for the satellite-derived and in-situ observations, respectively). Based on correlations, the FN05/K09/B10/BN07 simulation combining all of the activation mechanism updates has the best performance with the highest or second highest (after FN05/BN07 for the observational dataset) correlation with the two CDNC datasets.

Changes in CDNC produced by different aerosol activation schemes have a substantial impact on predicted cloud properties such as cloud fraction, optical thickness, liquid water path, and shortwave cloud forcing. Although all model simulations predict CF very well (with NMBs from −0.5 to 1.1 %), there is a consistent underprediction in polar regions and underprediction in the mid-latitudes and tropics (see Fig. 1), which compensates each other and results in an globally-averaged good performance. The correlation between satellite-derived and predicted CF is essentially the same for all simulations at ~ 0.71. Significant underpredictions occur in COT (with NMBs of −55.2 to −40.3 %) and LWP (with NMBs of −75.5 to −66.8 %) for all simulations, with the largest underpredictions occurring in polar regions (see Fig. 1). The COT and LWP underpredictions are consistent with those of Gettelman et al. (2010) and Liu et al. (2011) who found that the predictions are most sensitive to dust loading and attributed the CAM5 underpredictions to a severe underestimation of aerosol concentrations in CAM5 in the Arctic (and likely Antarctic) regions. The underpredictions in COT and LWP may be caused by limitations and uncertainties associated with the microphysics modules for resolved and cumulus clouds as well as the aerosol-cloud interaction treatments in the AR-G00. The underpredictions of COT and LWP at high latitudes may also be affected by MODIS overestimations related to 3-D effects in plane-parallel visible-near-infrared retrievals with low solar zenith angle (Seethala and Horváth, 2010). For the prediction of both COT and LWP, the inclusion of the FN05 scheme and updates reduces the underpredictions moderately but the poor correlation (< −0.14) remains unaffected. It is worth noting that the additional CDNC predicted by the FN05 scheme acts similarly to the anthropogenic aerosol indirect effect; increasing the aerosol activation fraction is equivalent to adding more aerosols in the calculation of cloud albedo





ACPD
13, 32291–32325, 2013

and cloud lifetime effects. Similar to CF, comparison of satellite-derived and predicted SWCF reveals that the FN05 scheme and updates change the sign of the prediction, from a slight underprediction (with an NMB of −1.4 %) for the AR-G00 simulation to moderate overpredictions (with NMBs from 11.3 to 13.1 %) for the FN05 series of simulations, increasing (more negative) the global average SWCF by −5.2 to −5.9 $W m^{-2}$. This is due to the combined increase in CF, COT, and LWP predicted by the FN05 scheme and updates. Despite worsening the bias, the inclusion of the FN05 updates improves the SWCF correlation slightly (from 0.88 to 0.89–0.91).

Despite having large underpredictions in LWP and COT, the AR-G00 has relatively accurate predictions of SWDOWN, LWDOWN, and OLR. The slight underpredictions of SWDOWN and LWDOWN (with NMBs of −2.3 and −1.1 % for SWDOWN and LWDOWN, respectively) in AR-G00 become slightly larger in the FN05 series of simulations (with NMBs of −6.1 to −5.2 % and −3.0 to −2.0 % for SWDOWN and LWDOWN). The overprediction of OLR for the AR-G00 simulation (with a NMB of 3.2 %), however, is reduced by the FN05 series of simulations. The underprediction of SWDOWN in the FN05 series of simulations is likely associated with the overprediction in CF. Because the transfer of longwave radiation is affected by COT and LWP more than CF, the improvement in these parameters by the FN05 series of simulations leads to moderate improvement in the longwave radiation parameters. Compared to the NCDC and NCEP-DOE Reanalysis-2 datasets, simulated T2 shows small underpredictions in the AR-G00 simulation (with NMBs of −10.8 and −5.0 %, respectively) made slightly larger (with NMBs of −20.1 to −16.7 % and −20.5 to −17.4 %, respectively) by the FN05 scheme and updates. The opposite occurs for precipitation, where overpredictions by the AR-G00 scheme (with an NMB of 11.0 %) are reduced by FN05 and updates (with NMBs of 8.5 to 9.1 %). Yang et al. (2013) found that the total precipitation in the tropics (−30° to 30°) simulated by CAM5 is most sensitive (among several key parameters in the Zhang–McFarlane deep convection scheme) to the (1) CAPE consumption time scale, (2) parcel fractional mass entrainment rate over ocean, and (3) radius of





ACPD
13, 32291–32325, 2013

detrained ice from deep convection, suggesting that changes to these values would optimize predictions.

### 3.2 Regional impacts of aerosol activation treatments

#### 3.2.1 Aerosol optical depth and cloud droplet number concentration

Like the global averages, the zonal average AOD differences between the simulations are relatively insensitive (differences < 0.01) to the choice of aerosol activate schemes. Much of the underprediction by all model simulations in the Southern Hemisphere from $-70^\circ$ to $-40^\circ$ is due to a bias in satellite products (i.e., MODIS Collection 5.1), which does not account for the wind speed-dependent whitecap and foam fraction on the ocean surface (Levy, 2013). Zonal-average CDNC, on the other hand, is very sensitive to the different activation schemes. The largest differences in CDNC predicted by the AR-G00 and FN05 series of simulations are in the mid-latitudes (from $-50^\circ$ to $-20^\circ$ and $20^\circ$ to $50^\circ$), where the AR-G00 underpredicts CDNC by 10 to 50 $cm^{-3}$ and the FN05 series of simulations overpredict CDNC by 25–50 $cm^{-3}$ compared to the MODIS-derived dataset. These under/overpredictions are not related to AOD (a proxy for aerosol abundance), which is relatively well predicted by all of the simulations compared to MODIS-derived AOD values in the mid-latitudes. Like the global average CDNC, the higher zonal CDNC in the FN05 series of simulations (relative to AR-G00) can be attributed to the different values of the effective uptake coefficient used in FN05 and AR-G00 (Zhang et al., 2012). Among the FN05 series of simulations, the zonal-average CDNC is the highest for the FN05, FN05/K09, and FN/BN07 simulations and the lowest (closer to the MODIS-derived values) for the FN05/B10 and FN05/K09/B10/BN07 simulations. The slightly higher global correlation between the satellite and model predicted CDNC for the FN05/K09 and FN05/K09/B10/BN07 simulations can be attributed to the higher CDNC from insoluble adsorption in regions with large dust emissions (centered around $-30^\circ$ for deserts in southern Africa, Australia, and Patagonia and $30^\circ$ for the Sahara, Arabian, and Sonoran Deserts). Figure 2 shows that CDNC predicted by the AR-G00





ACPD
13, 32291–32325, 2013

simulation is most similar to MODIS-derived CDNC over oceanic regions, while the FN05 series of simulations better predict CDNC over continental areas. This result is consistent with that of Fig. 3a, where a comparison of field campaign-observed CDNC and predictions from the AR-G00 and FN05/K09/B10/BN07 simulations reveals substantial improvement in FN05/K09/B10/BN07-predicted CDNC for continental regions which are significantly underpredicted in AR-G00. The large improvement (relative to AR-G00) in continental regions from the FN05/K09/B10/BN07 simulation results mainly from the higher activation fraction in the FN05 scheme and larger fraction of insoluble aerosols that can be activated in the K09 scheme (see Fig. 3a for comparison). The slight overpredictions in clean marine CDNC from the FN05 simulation do not occur in the FN05/K09/B10/BN07 simulation (see Fig. 3b) because of the inclusion of giant sea-salt aerosol activation kinetics which accounts for the slow condensation of water on these particles.

Separating the aerosol activation processes involved in the FN05/K09/B10/BN07 simulation shows that the processes have unequal impacts on CDNC resulting in distinct spatial distributions of column CDNC (Figs. 4 and 5). With the inclusion of the FN05 activation scheme, most areas (with the exception of desert regions in northern Africa, Arabian Peninsula, and Antarctica) experience an increase in column CDNC. The largest increases in column CDNC occur in regions near or downwind of population centers in China, US, and Europe. As a percentage, however, the largest changes occur in the Tibetan Plateau, western US, Greenland, and remote Pacific Ocean where CDNC is low. Globally, the average increase in CDNC from the AR-G00 simulation to the FN05 simulation is 170 %. While similar to FN05 in the magnitude of CDNC change from AR-G00, the FN05/K09 simulation has higher percentage changes in CDNC over many desert regions such the Saharan and Arabian Deserts leading to a global average increase of 178 %. This additional increase is the result of insoluble CCN activating into cloud droplets that would not activate according to Köhler theory on which the AR-G05 and FN05 are based. Accounting for the giant CCN activation kinetics in FN05/B10 leads to smaller changes in CDNC relative to AR-G00, especially over the remote ma-





ACPD
13, 32291–32325, 2013

rine and desert regions where sea-salt aerosol and dust are important CCN sources. Because of the large fraction of the Earth covered by oceans, the FN05/B10 scheme has a globally-significant impact on average column CDNC (the average increase from AR-G00 decreases from 170 % in FN05 to 139 % in FN05/B10). The inclusion of entrainment in the calculation of column CDNC from the FN05/BN07 simulation has a minor effect on the global average change compared to FN05, but does cause modest regional decreases in column CDNC over areas where convective clouds have high entrainment rates such as central Africa, Indonesia, South America, and the equatorial Pacific (see Fig. 5). Because only entrainment associated with deep convection affects aerosol activation in FN05/BN07 (and FN05/K09/B10/BN07), other areas have no entrainment effects and therefore mostly experience little change in column CDNC. Some areas (Kerguelen Plateau, equatorial north Pacific, equatorial Atlantic off the African coast) in the FN05/BN07 simulation have slightly increased CDNC relative to the FN05 simulation (see Fig. 5); this surprising result is possibly due to feedbacks from the online-coupled CESM/CAM5 where aerosol activation affects cloud microphysical processes (such as collision-coalescence) parameterized by Morrison and Gettelman (2008). CESM/CAM5 has the capability to simulate the feedbacks from meteorology back to aerosol activation (via changes in sea-salt and dust source functions with wind speed among others); however, analysis of the correlations between changes in column CDNC and surface meteorology/natural aerosol concentrations suggests that these feedbacks are not widespread (see Fig. S1). Both the FN05/K09 and FN05/B10 simulations also experience isolated regions in which the CDNC change is opposite to the expected (from box model simulations) trend; these areas are less widespread than FN05/BN07 because of the stronger global sensitivity of CDNC to insoluble adsorption and giant CCN activation kinetics. Areas experiencing the opposite change in CDNC than expected may be in transitional regimes as described by Reutter et al. (2009) where cloud droplet formation is sensitive to both aerosol activation and updraft velocity. Combined, the effects of insoluble adsorption, giant CCN activation kinetics, and entrainment lead to a predicted change in column CDNC from the FN05 scheme that





ACPD
13, 32291–32325, 2013

is higher than FN05 over desert regions, slightly lower over much of the ocean (see Figs. 4 and 5), and the same in some areas such as the continental US because of the compensating effects of insoluble adsorption and giant CCN activation kinetics. Compared with the AR-G00 simulation, the FN05/K09/B10/BN07 simulation combining all of the activation updates has a global average percent change in column CDNC of 155 %.

#### 3.2.2 Cloud fraction, cloud optical thickness, and liquid water path

Unlike CDNC which is sensitive to both the implementation of the FN05 scheme and the subsequent updates, changes in zonal-average CF, COT, and LWP are noticeable only by the transition from the AR-G00 to the FN05 series of simulations (see Fig. 1). Incremental changes are predicted for the CF predictions from different aerosol activation schemes, with the largest changes in the Arctic. Figure 1 shows that the large underpredictions in COT and LWP by AR-G00 for mid-latitude regions (30–60° N/S) are significantly improved by the implementation of the FN05 series of simulations. In tropical regions, the AR-G00 and all the FN05-based simulations have the lowest bias compared to satellite observations and there exists little difference between the model simulations, in particular in COT. The insensitivity of tropical cloud properties to the various aerosol activation parameterizations is likely due to the strong updrafts in the region which have been shown to have a lower variance in the activated fraction from different parameterizations than do weak updrafts (Ghan et al., 2011). Like CF, all simulated COT and LWP are most different from MODIS-derived values in polar regions because of the influence of radiatively active snow on overlying cloud fraction (Kay et al., 2012) and MODIS overestimations of cloud optical properties at high latitudes related to 3-D effects in plane-parallel visible-near-infrared retrievals with low solar zenith angles (Seethala and Horváth, 2010). Predictions of CF, COT, and LWP in the AR-G00 and FN05 series of simulations are most different in polar regions because of the sensitivity of Arctic and Antarctic CDNC (and corresponding cloud properties) to slight changes in aerosol number (Moore et al., 2013). Mixed-phase clouds, which are found in polar





ACPD
13, 32291–32325, 2013

regions, are particularly sensitive because they are affected by both aerosol activation and ice nucleation (Lance et al., 2011; Xie et al., 2013). Ignoring polar regions which have mixed-phase clouds, the moderate underpredictions of CF, COT, and LWP in the AR-G00 are consistently reduced in the FN05 series of simulations.

### 3.2.3 Shortwave cloud forcing, surface solar radiation, temperature, and precipitation

Changes in CF, COT, and LWP affect the predicted climatic impact of aerosols, as shown by the changes in SWCF, surface incoming shortwave radiation, temperature, and precipitation in Figs. 4 and 6 and 7. The difference in SWCF between the AR-G00 and FN05 simulations is the highest in the mid-latitudes where the large CDNC differences occur. In mid-latitude regions from $-60^{\circ}$ to $-30^{\circ}$, the transition from the AR-G00 to the FN05 activation schemes changes the sign of the model bias from negative to positive. Globally, the largest changes in SWCF and surface incoming shortwave radiation between the AR-G00 and FN05 simulations occur over the oceans, where widespread areas experience a 25 % increase (more negative) in SWCF and 10 % decrease in surface incoming solar radiation (see Fig. 4). This sensitivity of radiative forcing in oceanic regions to aerosol activation is due to two main reasons: (1) the low penetration of shortwave radiation through stratocumulus decks covering large areas of the ocean and (2) the sensitivity of marine cloud albedo to changes in CDNC (Twomey, 1991; Platnick and Twomey, 1994; Moore et al., 2013). The updates to the FN05 scheme do not substantially change the spatial distribution of the surface shortwave radiation relative to the change from AR-G00 to FN05 (see Figs. 4 and 6). The sign of the surface shortwave radiation changes is inversely related to that of the SWCF changes for most regions, particularly in the northern Pacific, Atlantic, and southern Oceans.

Like surface incoming solar radiation, the change in T2 between the AR-G00 and FN05 is negative over most areas with the exception of desert and ice-covered areas (see Fig. 4) whose surface albedo is high. Among the FN05 series of simulations (see

Fig. 7), two regions show noticeable differences in T2 changes from FN05: (1) the Sahara/Gobi Deserts where T2 decreases in FN05/K09 (with insoluble adsorption) and FN05/B10 (with giant CCN activation kinetics) simulations and (2) the tropical Pacific Ocean where T2 increases in the FN05/B10 and FN05/BN07 (with entrainment effects) simulations. As shown in Fig. 4, the changes in precipitation between AR-G00 and the FN05 series simulations exhibit more spatial variability than in the surface shortwave radiation and temperature fields, with few widespread areas having a consistent sign of change. The global average precipitation change from the AR-G00 to FN05 series of simulations is consistently negative, suggesting that CESM/CAM5 is simulating the cloud lifetime effect where increased CDNC leads to a decrease in cloud droplet radii and a subsequent suppression (for a majority of areas) in the precipitation rate. The effects of the combined updates of aerosol activation (i.e., insoluble adsorption, giant CCN activation kinetics, and entrainment) in the FN05/K09/B10/BN07 simulation, lead to a predicted change in temperature and precipitation from the AR-G00 scheme of $-0.9\,^{\circ}\mathrm{C}$ and $-0.04\,\mathrm{mm\,day^{-1}}$, respectively.

## 4 Conclusions

In this study, several process-based aerosol activation schemes are implemented into the Community Atmosphere Model version 5.1.1 within the Community Earth System Model version 1.0.5 (CESM/CAM5) to determine the global impacts of individual activation processes on cloud properties and meteorology. Compared to simulations using the AR-G00 scheme, simulations with the FN05 series of schemes which account for entrainment, insoluble adsorption, and giant CCN typically have improved model predictions of cloud droplet number concentration, cloud optical thickness, and liquid water path. Individually, the inclusion of these updates leads to the following changes; (1) insoluble adsorption increases CDNC over desert regions and (2) giant CCN activation kinetics decreases CDNC over oceanic regions. The inclusion of entrainment in CESM/CAM5 leads to increases and decreases in regional CDNC, a result differ-





ACPD
13, 32291–32325, 2013

ent than the expected (from box model simulations) decrease which may be explained by feedbacks between aerosol activation and cloud microphysics. As CESM/CAM5 is an online-coupled model, complete attribution of the changes between simulations to a single mechanism (such as aerosol activation) is difficult due to these feedbacks. Further sensitivity studies on the interactions between aerosol activation and cloud microphysics using cloud parcel models, large eddy simulations, or global models simulating climatic time scales (decades or more) may be necessary to better understand these feedbacks. The increase in CDNC predicted by the simulations with the FN05-based schemes leads to an increase (more negative) in the global-average shortwave cloud forcing and a decrease in the surface shortwave radiation, near-surface temperature, and precipitation. The more accurate prediction of CDNC, cloud optical thickness, and liquid water path (based on improved NMBs and correlations relative to satellite and in-situ datasets) suggests that these physically-based updates better represent cloud activation in CESM/CAM5 and increase confidence in the prediction of the aerosol indirect effects.

**Supplementary material related to this article is available online at http://www.atmos-chem-phys-discuss.net/13/32291/2013/acpd-13-32291-2013-supplement.pdf.**

*Acknowledgements.* This project is sponsored by the National Science Foundation EaSM program (AGS-1049200). AN acknowledges support from DOE EaSM and NASA MAP grants. Thanks are due to R. Bennartz, Department of Atmospheric and Oceanic Sciences, University of Wisconsin-Madison, for providing derived CDNC data derived based on MODIS measurements. The GPCP combined precipitation data were developed and computed by the NASA/Goddard Space Flight Center's Laboratory for Atmospheres as a contribution to the GEWEX Global Precipitation Climatology Project. We would like to acknowledge high-performance computing support from Yellowstone (ark:/85065/d7wd3xhc) provided by NCAR's Computational and Information Systems Laboratory, sponsored by the National Science Foundation.





ACPD
13, 32291–32325, 2013



Title Page
Abstract | Introduction
Conclusions | References
Tables | Figures
◀| |▶
◀ ▶
Back | Close
Full Screen / Esc
Printer-friendly Version
Interactive Discussion

## References


Abdul-Razzak, H. and Ghan, S. J.: A parameterization of aerosol activation: 2. multiple aerosol types, J. Geophys. Res., 105, 6837–6844, 2000.

Abdul-Razzak, H., Ghan, S., and Rivera-Carpio, C.: A parameterisation of aerosol activation, Part I: single aerosol type, J. Geophys. Res., 103, 6123–6132, doi:10.1029/97JD03735, 1998.

Albrecht, B. A.: Aerosols, cloud microphysics, and fractional cloudiness, Science, 245, 1227–1230, doi:10.1126/science.245.4923.1227, 1989.

Barahona, D. and Nenes, A.: Parameterization of cloud droplet formation in large-scale models: including effects of entrainment, J. Geophys. Res., 112, D16206, doi:10.1029/2007JD008473, 2007.

Barahona, D., West, R. E. L., Stier, P., Romakkaniemi, S., Kokkola, H., and Nenes, A.: Comprehensively accounting for the effect of giant CCN in cloud activation parameterizations, Atmos. Chem. Phys., 10, 2467–2473, doi:10.5194/acp-10-2467-2010, 2010.

Bennartz, R.: Global assessment of marine boundary layer cloud droplet number concentration from satellite, J. Geophys. Res.-Atmos., 112, D02201, doi:10.1029/2006JD007547, 2007.

Chuang, P. Y., Charlson, R. J., and Seinfeld, J. H.: Kinetic limitations on droplet formation in clouds, Nature, 390, 594–596, doi:10.1038/37576, 1997.

Forster, P., Ramaswamy, V., Artaxo, P., Berntsen, T., Betts, R., Fahey, W. D., Haywood, J., Lean, J., Lowe, D. C., Myhre, G., Nganga, J., Prinn, R., Raga, G., Schultz, M., and Van Dorland, R.: Changes in atmospheric constituents and in radiative forcing, in: Climate Change 2007: The Physical Science Basis, Contribution of Working Group 1 to the Fourth Assessment Report of the Intergovernmental Panel on Climate Change, Cambridge University Press, Cambridge, UK and New York, NY, 129–234, 2007.

Fountoukis, C. and Nenes, A.: Continued development of a cloud droplet formation parameterization for global climate models, J. Geophys. Res., 110, D11212, doi:10.1029/2004jd005591, 2005.

Gettelman, A., Liu, X., Ghan, S. J., Morrison, H., Park, S., Conley, A. J., Klein, S. A., Boyle, J., Mitchell, D. L., and Li, J. L. F.: Global simulations of ice nucleation and ice supersaturation with an improved cloud scheme in the Community Atmosphere Model, J. Geophys. Res., 115, D18216, doi:10.1029/2009jd013797, 2010.

Ghan, S. J., Abdul-Razzak, H., Nenes, A., Ming, Y., Liu, X., Ovchinnikov, M., Shipway, B., Mekhidze, N., Xu, J., and Shi, X.: Droplet nucleation: physically-based parameterizations and comparative evaluation, J. Adv. Model. Earth Syst., 3, M10001, doi:10.1029/2011MS000074, 2011.

Guenther, A., Karl, T., Harley, P., Wiedinmyer, C., Palmer, P. I., and Geron, C.: Estimates of global terrestrial isoprene emissions using MEGAN (Model of Emissions of Gases and Aerosols from Nature), Atmos. Chem. Phys., 6, 3181–3210, doi:10.5194/acp-6-3181-2006, 2006.

He, J. and Zhang, Y.: Improvement and further development in CESM/CAM5: gas-phase chemistry and inorganic aerosol treatments, Atmos. Chem. Phys. Discuss., 13, 27717–27777, doi:10.5194/acpd-13-27717-2013, 2013.

Heald, C. L., Henze, D. K., Horowitz, L. W., Feddema, J., Lamarque, J. F., Guenther, A., Hess, P. G., Vitt, F., Seinfeld, J. H., Goldstein, A. H., and Fung, I.: Predicted change in global secondary organic aerosol concentrations in response to future climate, emissions, and land use change, J. Geophys. Res.-Atmos., 113, D05211, doi:10.1029/2007JD009092, 2008.

Karamchandani, P., Zhang, Y., Chen, S. Y., and Balmori-Bronson, R.: Development and testing of an extended chemical mechanism for global through-urban applications, Atmos. Pollut. Res., 3, 1–24, doi:10.5094/APR.2011.047, 2012.

Karydis, V. A., Kumar, P., Barahona, D., Sokolik, I. N., and Nenes, A.: On the effect of dust particles on global cloud condensation nuclei and cloud droplet number, J. Geophys. Res., 116, D23204, doi:10.1029/2011jd016283, 2011.

Kay, J. E., Hillman, B. R., Klein, S. A., Zhang, Y., Medeiros, B., Pincus, R., Gettelman, A., Eaton, B., Boyle, J., Marchand, R., and Ackerman, T. P.: Exposing global cloud biases in the Community Atmosphere Model (CAM) using satellite observations and their corresponding instrument simulators, J. Climate, 25, 5190–5207, doi:10.1175/JCLI-D-11-00469.1, 2012.

Khain, A. P., BenMoshe, N., and Pokrovsky, A.: Factors determining the impact of aerosols on surface precipitation from clouds: an attempt at classification, J. Atmos. Sci., 65, 1721–1748, 2008.

Köhler, H.: The nucleus in the growth of hygroscopic droplets, T. Faraday Soc., 32, 1152–1161, 1936.

Kumar, P., Sokolik, I. N., and Nenes, A.: Parameterization of cloud droplet formation for global and regional models: including adsorption activation from insoluble CCN, Atmos. Chem. Phys., 9, 2517–2532, doi:10.5194/acp-9-2517-2009, 2009.

Lance, S., Shupe, M. D., Feingold, G., Brock, C. A., Cozic, J., Holloway, J. S., Moore, R. H., Nenes, A., Schwarz, J. P., Spackman, J. R., Froyd, K. D., Murphy, D. M., Brioude, J., Cooper, O. R., Stohl, A., and Burkhart, J. F.: Cloud condensation nuclei as a modulator of ice processes in Arctic mixed-phase clouds, Atmos. Chem. Phys., 11, 8003–8015, doi:10.5194/acp-11-8003-2011, 2011.

Leaitch, W. R., Isaac, G. A., Strapp, J. W., Banic, C. M., and Wiebe, H. A.: The relationship between cloud droplet number concentrations and anthropogenic pollution: observations and climatic implications, J. Geophys. Res., 97, 2463–2474, doi:10.1029/91JD02739, 1992.

Levy, R. C., Mattoo, S., Munchak, L. A., Remer, L. A., Sayer, A. M., and Hsu, N. C.: The Collection 6 MODIS aerosol products over land and ocean, Atmos. Meas. Tech. Discuss., 6, 159–259, doi:10.5194/amtd-6-159-2013, 2013.

Liu, X., Xie, S., Boyle, J., Klein, S. A., Shi, X., Wang, Z., Lin, W., Ghan, S. J., Earle, M., Liu, P. S. K., and Zelenyuk, A.: Testing cloud microphysics parameterizations in NCAR CAM5 with ISDAC and M-PACE observations, J. Geophys. Res., 116, D00T11, doi:10.1029/2011JD015889, 2011.

Mårtensson, E., Nilsson, E., de Leeuw, G., Cohen, L., and Hansson, H.-C.: Laboratory simulations and parameterisation of the primary marine aerosol production, J. Geophys. Res., 108, 4297, doi:10.1029/2002JD002263, 2003.

Martin, G. M., Johnson, D. W., and Spice, A.: The measurement and parameterization of effective radius of droplets in warm stratocumulus clouds, J. Atmos. Sci., 51, 1823–1842, 1994.

Merikanto, J., Napari, I., Vehkamaki, H., Anttila, T., and Kulmala, M.: New parameterization of sulfuric acid-ammonia-water ternary nucleation rates at tropospheric conditions, J. Geophys. Res., 112, D15207, doi:10.1029/2006JD007977, 2007.

Monahan, E., Spiel, D., and Davidson, K.: A model of marine aerosol generation via white caps and wave disruption, in: Oceanic Whitecaps, edited by: Monahan, E. and MacNiochaill, G., Reidel, Dordrecht, the Netherlands, 167–193, 1986.

Moore, R. H., Karydis, V. A., Capps, S. L., Lathem, T. L., and Nenes, A.: Droplet number uncertainties associated with CCN: an assessment using observations and a global model adjoint, Atmos. Chem. Phys., 13, 4235–4251, doi:10.5194/acp-13-4235-2013, 2013.

Morrison, H. and Gettelman, A.: A new two-moment bulk stratiform cloud microphysics scheme in the Community Atmosphere Model, Version 3 (CAM3), part I: description and numerical tests, J. Climate, 21, 3642–3659, doi:10.1175/2008JCLI2105.1, 2008.





ACPD
13, 32291–32325, 2013

Incorporation of advanced aerosol activation treatments into CESM/CAM5

B. Gantt et al.

Neale, R. B., Chen, C.-C., Gettelman, A., Lauritzen, P. H., Park, S., Williamson, D. L., Conley, A. J., Garcia, R., Kinnison, D., Lamarque, J.-F., Marsh, D., Mills, M., Smith, A. K., Tilmes, S., Vitt, F., Morrison, H., Cameron-Smith, P., Collins, W. D., Iacono, M. J., Easter, R. C., Liu, X., and Taylor, M. A.: Description of the NCAR Community Atmosphere Model (CAM 5.0), Tech. rep., National Center for Atmospheric Research, National Center for Atmospheric Research, Boulder, CO, 2010.

Nenes, A. and Seinfeld, J. H.: Parameterization of cloud droplet formation in global climate models, J. Geophys. Res., 108, 4415, doi:10.1029/2002jd002911, 2003.

Nenes, A., Ghan, S., Abdul-Razzak, H., Chuang, P. Y., and Seinfeld, J. H.: Kinetic limitations on cloud droplet formation and impact on cloud albedo, Tellus B, 53, 133–149, doi:10.1034/j.1600-0889.2001.d01-12.x, 2001.

Petters, M. D. and Kreidenweis, S. M.: A single parameter representation of hygroscopic growth and cloud condensation nucleus activity, Atmos. Chem. Phys., 7, 1961–1971, doi:10.5194/acp-7-1961-2007, 2007.

Platnick, S. and Twomey, S.: Determining the susceptibility of cloud albedo to changes in droplet concentration with the advanced very high resolution radiometer, J. Appl. Meteorol., 33, 334–347, doi:10.1175/1520-0450(1994)033<0334:DTSOCA>2.0.CO;2, 1994.

Ramanathan, V., Crutzen, P. J., Kiehl, J. T., and Rosenfeld, D.: Aerosols, climate, and the hydrological cycle, Science, 294, 2119–2124, doi:10.1126/science.1064034, 2001.

Rosenfeld, D., Lohmann, U., Raga, G. B., O'Dowd, C. D., Kulmala, M., Fuzzi, S., Reissell, A., and Andreae, M. O.: Flood or drought: how do aerosols affect precipitation?, Science, 321, 1309–1313, 2008.

Reutter, P., Su, H., Trentmann, J., Simmel, M., Rose, D., Gunthe, S. S., Wernli, H., Andreae, M. O., and Pöschl, U.: Aerosol- and updraft-limited regimes of cloud droplet formation: influence of particle number, size and hygroscopicity on the activation of cloud condensation nuclei (CCN), Atmos. Chem. Phys., 9, 7067–7080, doi:10.5194/acp-9-7067-2009, 2009.

Seethala, C. and Horvath, Á.: Global assessment of AMSR-E and MODIS cloud liquid water path retrievals in warm oceanic clouds, J. Geophys. Res., 115, D13202, doi:10.1029/2009JD012662, 2010.

Twomey, S.: Pollution and the planetary albedo, Atmos. Environ., 8, 1251–1256, doi:10.1016/0004-6981(74)90004-3, 1974.

Twomey, S.: Influence of pollution on shortwave albedo of clouds, J. Atmos. Sci., 34, 1149–1152, doi:10.1175/1520-0469(1977)034<1149:TIOPOT>2.0.CO;2, 1977.






ACPD
13, 32291–32325, 2013

Twomey, S.: Aerosols, clouds and radiation, Atmos. Environ., 25, 2435–2442, doi:10.1016/0960-1686(91)90159-5, 1991.
Vehkamäki, H., Kulmala, M., Napari, I., Lehtinen, K. E. J., Timmreck, C., Noppel, M., and Laaksonen, A.: An improved parameterization for sulfuric acid water nucleation rates for tropospheric and stratospheric conditions, J. Geophys. Res., 107, 4622–4632, doi:10.1029/2002JD002184, 2002.
Wang, M., Penner, J. E., and Liu, X.: Coupled IMPACT aerosol and NCAR CAM3 model: evaluation of predicted aerosol number and size distribution, J. Geophys. Res., 114, D06302, doi:10.1029/2008JD010459, 2009.
Xie, S., Liu, X., Zhao, C., Zhang, Y.: Sensitivity of CAM5-simulated arctic clouds and radiation to ice nucleation parameterization, J. Climate, 26, 5981–5999, doi:10.1175/JCLI-D-12-00517.1, 2013.
Yang, B., Qian, Y., Lin, G., Leung, L.-Y., Rasch, P. J., Zhang, G. J., McFarlane, S. A., Zhao, C., Zhang, Y., Wang, H., Wang, M., Liu, X.: Uncertainty quantification and parameter tuning in the CAM5 Zhang–McFarlane convection scheme and impact of improved convection on the global circulation and climate, J. Geophys. Res. Atmos., 118, 395–415, doi:10.1029/2012JD018213, 2013.
Yu, F.: Ion-mediated nucleation in the atmosphere: Key controlling parameters, implications, and look-up table, J. Geophys. Res., 115, D03206, doi:10.1029/2009JD012630, 2010.
Zender, C., Bian, H., and Newman, D.: Mineral Dust Entrainment and Deposition (DEAD) model: description and 1990s dust climatology., J. Geophys. Res., 108, 4416–4437, doi:10.1029/2002jd002775, 2003.
Zhang, G. J. and McFarlane, N. A.: Sensitivity of climate simulations to the parameterization of cumulus convection in the Canadian Climate Centre general circulation model, Atmos. Ocean, 33, 407–446, 1995.
Zhang, Y.: Online-coupled meteorology and chemistry models: history, current status, and outlook, Atmos. Chem. Phys., 8, 2895–2932, doi:10.5194/acp-8-2895-2008, 2008.
Zhang, Y., Karamchandani, P., Glotfelty, T., Streets, D. G., Skamarock, W. C., Grell, G., Nenes, A., Yu, F., and Bennartz, R.: Development and initial application of the Global-Through-Urban Weather Research and Forecasting Model with Chemistry (GU-WRF/Chem), J. Geophys. Res., 117, D20206, doi:10.1029/2012JD017966, 2012.





ACPD
13, 32291–32325, 2013

Incorporation of advanced aerosol activation treatments into CESM/CAM5

B. Gantt et al.

**Table 1.** The CESM/CAM5-MAM7 simulations performed in this study.

| Name | Köhler activation | Population spitting | Insoluble adsorption | Giant CCN equilibrium | Entrainment effects | Major Differences and Purpose |
|---|---|---|---|---|---|---|
| AR-G00 | √ | | | | | Baseline simulation |
| FN05 | √ | √ | | | | Uses the Fountoukis and Nenes (2005) activation scheme |
| FN05/K09 | √ | √ | √ | | | Uses the Fountoukis and Nenes (2005) activation scheme updated by Kumar et al. (2009), accounting for the impact of insoluble adsorption |
| FN05/B10 | √ | √ | | √ | | Uses the Fountoukis and Nenes (2005) activation scheme updated by Barahona et al. (2010), accounting for the impact of giant CCN activation kinetics |
| FN05/BN07 | √ | √ | | | √ | Uses the Fountoukis and Nenes (2005) activation scheme updated by Barahona and Nenes (2007), accounting for the impact of dynamic entrainment |
| FN05/K09/B10/BN07 | √ | √ | √ | √ | √ | Uses the Fountoukis and Nenes (2005) activation scheme updated by Kumar et al. (2009), Barahona et al. (2010), and Barahona and Nenes (2007), accounting for all above aerosol activation processes |





ACPD
13, 32291–32325, 2013

**Table 2.** Annual mean normalized mean biases (NMBs, in %) of the CESM-CAM5-predicted meteorological/radiative variables.

| Variable | Dataset | AR-G00 | FN05 | FN05/K09 | FN05/B10 | FN05/BN07 | FN05/K09/B10/BN07 |
|---|---|---|---|---|---|---|---|
| AOD | MODIS | −34.0 | −32.3 | −31.7 | −30.8 | −31.2 | −31.8 |
| CDNC | Bennartz (2007) | −40.8 | 28.0 | 37.4 | 10.2 | 30.0 | 16.8 |
| | Karydis et al. (2011) | −71.7 | −23.5 | −21.5 | −40.6 | −21.9 | −34.3 |
| CF | MODIS | −0.5 | 0.5 | 0.9 | 0.7 | 1.1 | 0.7 |
| COT | MODIS | −55.2 | −41.1 | −40.3 | −43.0 | −41.9 | −41.5 |
| LWP | MODIS | −75.5 | −66.9 | −66.8 | −67.8 | −67.3 | −67.0 |
| SWCF | CERES | −1.4 | 13.0 | 13.1 | 11.3 | 12.1 | 12.0 |
| SWDOWN | BSRN | −2.3 | −5.3 | −6.1 | −5.4 | −5.3 | −5.2 |
| LWDOWN | BSRN | −1.1 | −3.0 | −2.5 | −2.4 | −2.0 | −2.4 |
| OLR | NOAA-CDC | 3.2 | 2.2 | 2.2 | 2.3 | 2.4 | 2.4 |
| T2 | NCDC | −10.8 | −20.1 | −19.7 | −18.8 | −16.7 | −18.8 |
| | NCEP-DOE Reanalysis-2 | −5.0 | −20.5 | −19.9 | −18.3 | −17.4 | −18.6 |
| Precipitation | GPCP | 11.0 | 8.5 | 8.7 | 8.9 | 8.8 | 9.1 |
| WS10 | NCDC | −15.4 | −15.2 | −14.7 | −15.2 | −14.8 | −15.4 |





ACPD
13, 32291–32325, 2013

**Table 3.** Annual mean correlation coefficients of the CESM-CAM5-predicted meteorological/radiative variables.

| Variable | Dataset | AR-G00 | FN05 | FN05/K09 | FN05/B10 | FN05/BN07 | FN05/K09/B10/BN07 |
|---|---|---|---|---|---|---|---|
| AOD | MODIS | 0.64 | 0.65 | 0.65 | 0.65 | 0.66 | 0.63 |
| CDNC | Bennartz (2007) | 0.49 | 0.55 | 0.58 | 0.55 | 0.56 | 0.60 |
| | Karydis et al. (2011) | 0.03 | 0.16 | 0.24 | 0.10 | 0.39 | 0.36 |
| CF | MODIS | 0.71 | 0.72 | 0.71 | 0.71 | 0.70 | 0.71 |
| COT | MODIS | −0.19 | −0.16 | −0.15 | −0.14 | −0.15 | −0.14 |
| LWP | MODIS | −0.38 | −0.37 | −0.37 | −0.36 | −0.37 | −0.37 |
| SWCF | CERES | 0.88 | 0.90 | 0.89 | 0.90 | 0.91 | 0.90 |
| SWDOWN | BSRN | 0.91 | 0.91 | 0.91 | 0.90 | 0.91 | 0.91 |
| LWDOWN | BSRN | 0.98 | 0.97 | 0.98 | 0.98 | 0.98 | 0.98 |
| OLR | NOAA-CDC | 0.97 | 0.97 | 0.97 | 0.97 | 0.97 | 0.97 |
| T2 | NCDC | 0.93 | 0.94 | 0.93 | 0.93 | 0.93 | 0.93 |
| | NCEP-DOE Reanalysis-2 | 0.99 | 0.99 | 0.99 | 0.99 | 0.99 | 0.99 |
| Precipitation | GCPC | 0.77 | 0.76 | 0.77 | 0.78 | 0.80 | 0.78 |
| WS10 | NCDC | 0.41 | 0.41 | 0.41 | 0.41 | 0.41 | 0.41 |





ACPD
13, 32291–32325, 2013

Discussion Paper | Discussion Paper | Discussion Paper | Discussion Paper |

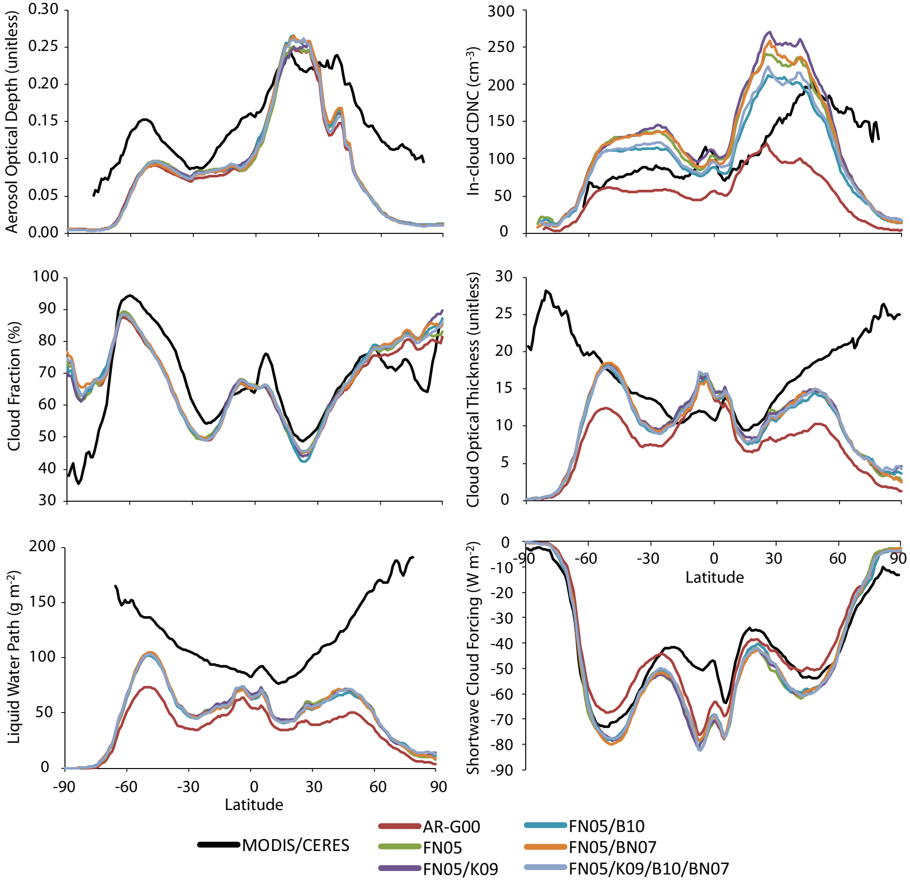


**Fig. 1.** Annual-average zonal-mean AOD, CDNC, CF, COT, LWP, and SWCF derived from satellites and predicted by CESM/CAM5.



ACPD
13, 32291–32325, 2013

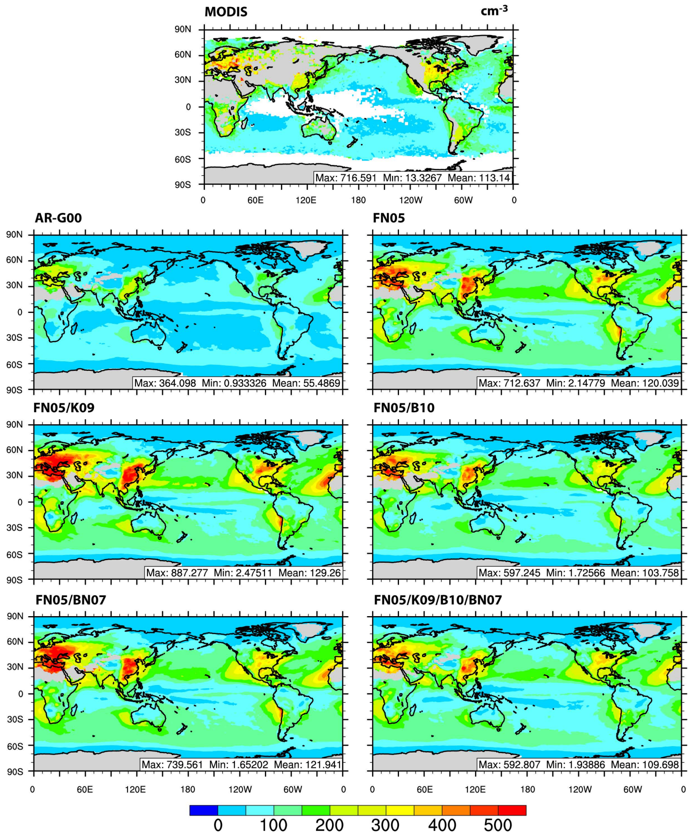


**Fig. 2.** Annual average low-level CDNC from MODIS (Bennartz, 2007) and CESM/CAM5 simulations.





ACPD
13, 32291–32325, 2013

Incorporation of advanced aerosol activation treatments into CESM/CAM5

B. Gantt et al.

Title Page
Abstract | Introduction
Conclusions | References
Tables | Figures
◀| |▶
◀ ▶
Back | Close
Full Screen / Esc
Printer-friendly Version
Interactive Discussion

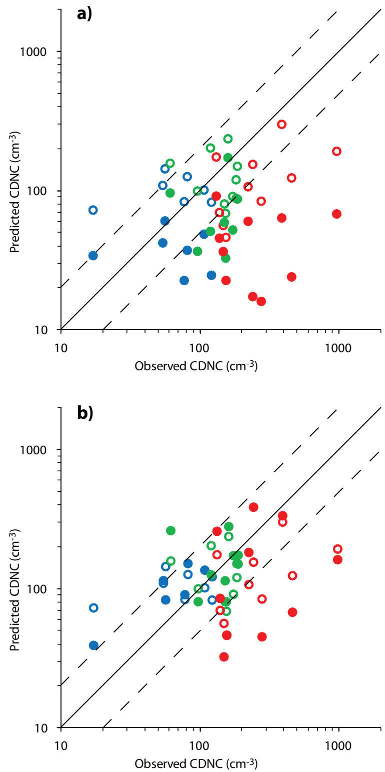


**Fig. 3.** Comparison of CESM/CAM5-predicted (at ∼ 930 mb) and observed low-level CDNC from clean marine (blue), polluted marine (green), and continental (red) as classified and summarized by Karydis et al. (2011). The filled circles are for the **(a)** AR-G00 and **(b)** FN05 simulations and hollow circles for the FN05/K09/B10/BN07 simulation. Observations for which the any of the simulations predicted CDNC < 10 $cm^{-3}$ were not included. The 1 : 1 and 1 : 2/2 : 1 lines are the solid and dotted black lines, respectively.





ACPD
13, 32291–32325, 2013

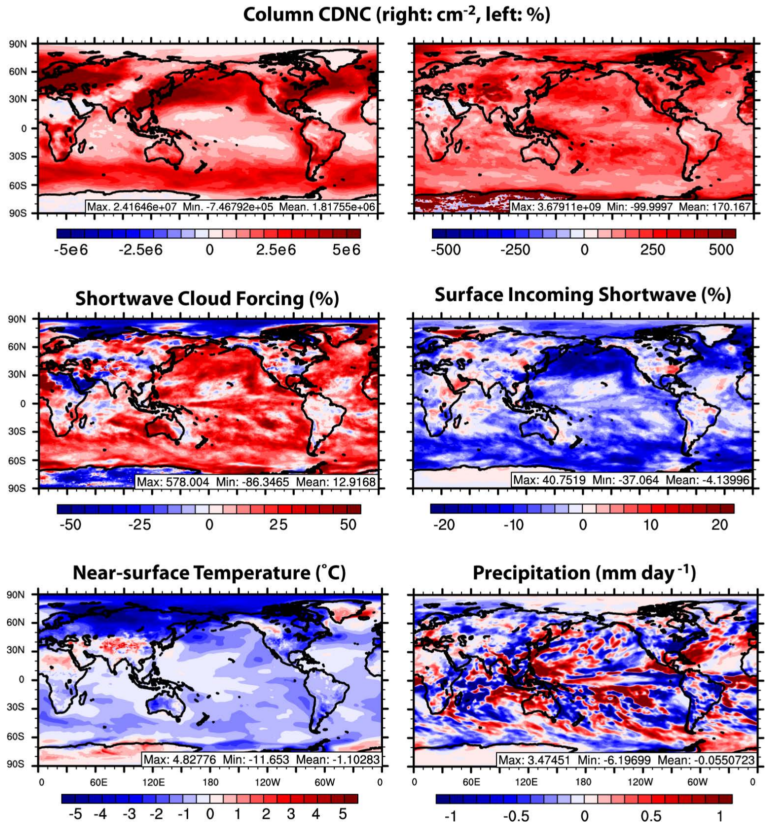


**Fig. 4.** Annual-average changes in column CDNC (absolute and percentage), shortwave cloud forcing, incoming shortwave radiation at the surface, near-surface temperature, and precipitation between the FN05 and AR-G00 CESM/CAM5 simulations.



Discussion Paper | Discussion Paper | Discussion Paper | Discussion Paper |

ACPD
13, 32291–32325, 2013

Incorporation of advanced aerosol activation treatments into CESM/CAM5

B. Gantt et al.

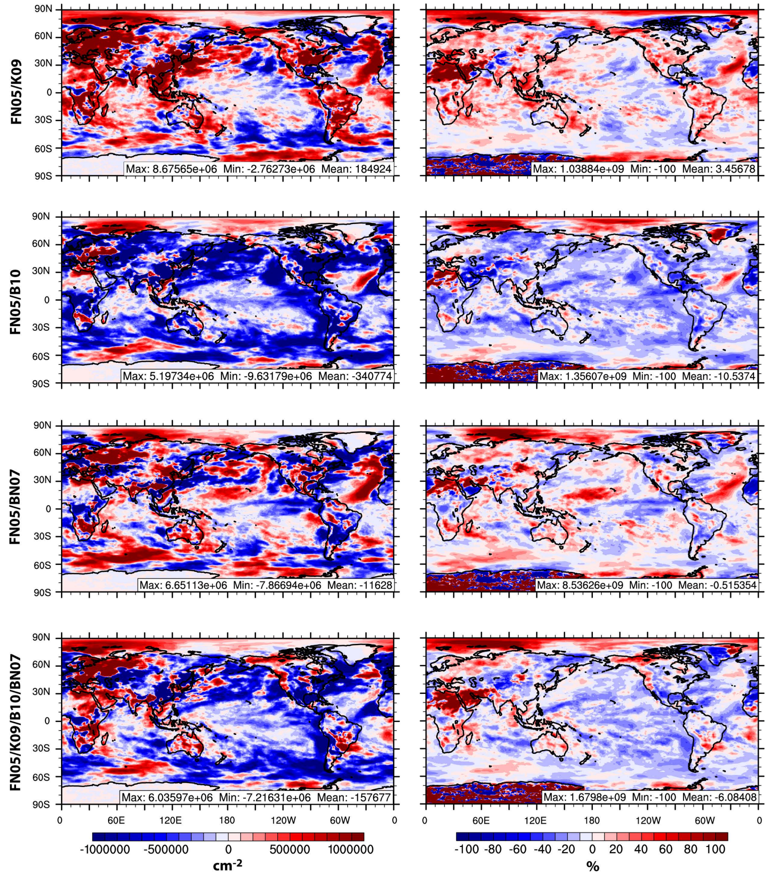


**Fig. 5.** Annual-average absolute (left, in units of $cm^{-2}$) and percentage (right) change in column CDNC from FN05 to each of the FN05 updates in CESM/CAM5.

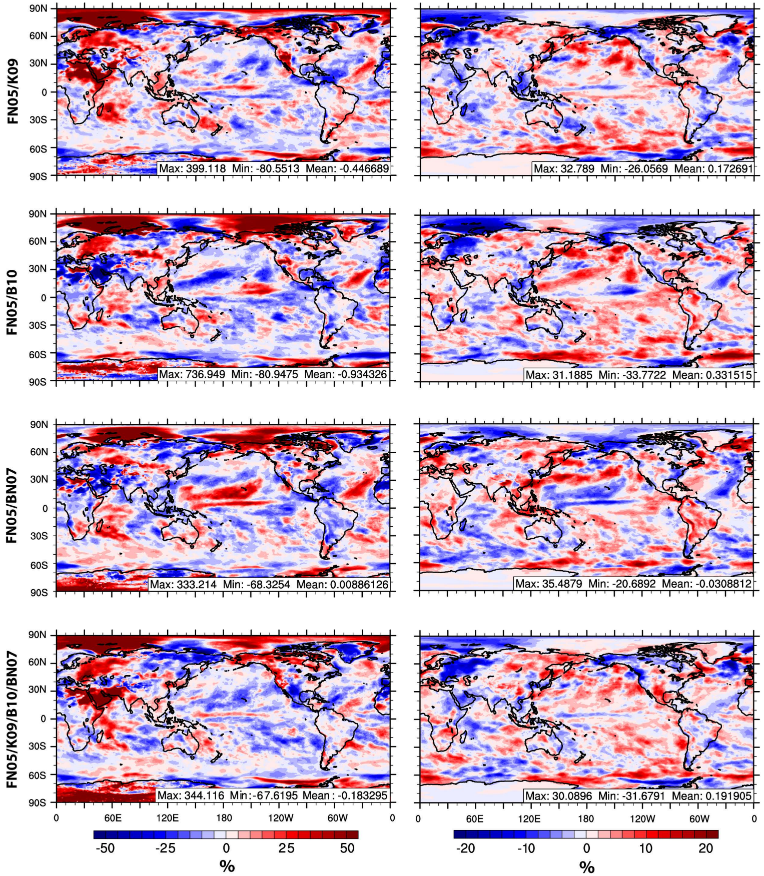


**Fig. 6.** Percentage changes in the annual average shortwave cloud forcing (left) and surface incoming shortwave radiation (right) from FN05 to each of the FN05 updates in CESM/CAM5.





ACPD
13, 32291–32325, 2013

Incorporation of advanced aerosol activation treatments into CESM/CAM5

B. Gantt et al.

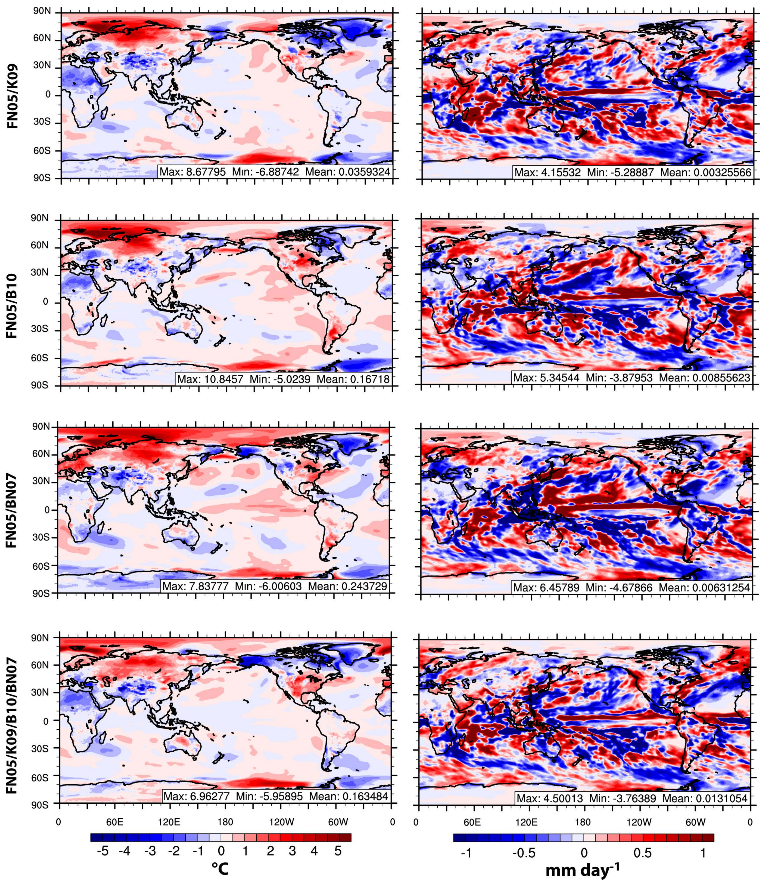


**Fig. 7.** Absolute change in the annual average near-surface temperature (left) and daily precipitation (right) from FN05 to each of the FN05 updates in CESM/CAM5.





ACPD
13, 32291–32325, 2013

Incorporation of advanced aerosol activation treatments into CESM/CAM5

B. Gantt et al.